MOUNTAIN-PLAINS CONSORTIUM

MPC 24-546 | Y.J. Kim

TRANSITION OF ALLOWABLE STRESS RATING TO LOAD AND RESISTANCE FACTOR RATING FOR TIMBER BRIDGES

MOUNTAIN-PLAINS CONSORTIUM REGION 8

A University Transportation Center sponsored by the U.S. Department of Transportation serving the Mountain-Plains Region. Consortium members:

Colorado State University
North Dakota State University
South Dakota State University
University of Colorado Denver
University of Denver
University of Utah
Utah State University
University of Wyoming

Technical Report Documentation Page

1. Report No.	2. Government Accession No.	3. Recipient's Catalog No.
MPC-675		

4. Title and Subtitle	5. Report Date
Transition of Allowable Stress Rating to Load and Resistance Factor Rating for Timber Bridges	August 2024
	6. Performing Organization Code

7. Author(s)	8. Performing Organization Report No.
Yale Jimmy Kim	MPC 24-546

9. Performing Organization Name and Address	10. Work Unit No. (TRAIS)
University of Colorado Denver 1200 Larimer Street Denver, CO, 80217	11. Contract or Grant No.

12. Sponsoring Agency Name and Address	13. Type of Report and Period Covered
Mountain-Plains Consortium North Dakota State University PO Box 6050, Fargo, ND 58108	Final Report
	14. Sponsoring Agency Code

15. Supplementary Notes

Supported by a grant from the US DOT, University Transportation Centers Program

16. Abstract

This report presents the relevancy of the allowable stress rating (ASR) and the load and resistance factor rating (LRFR) methods for timber bridges. Benchmark bridges constructed in the 1930s have been upgraded with hollow structural steel (HSS) beams and three-dimensional finite element models provide technical information necessary for examining their behavior and rating evaluations. Complying with published manuals, 17 rating vehicles are considered across three categories (design, legal, and permit) to generate the maximum responses of the bridges. The vehicles' position dominates the deflection profiles of the unrepaired bridges. After installing the HSS beams, the live loads are redistributed, and stiffness enhancement is noticed in the transverse direction of the bridges. The rating factors calculated with ASR exceed those with LRFR for the unrepaired bridges regardless of vehicle configurations, and the level of disparity between these rating approaches increases when the bridges are repaired owing to differences in load factors. In terms of sensitivity to average daily truck traffic, the LRFR factors of the bridges under the "legal" vehicles are more responsive than the factors subjected to other vehicle types. From a probability perspective, the compatibility of these rating methodologies varies contingent upon vehicle categories and the presence of the HSS beams. Practice guidelines are proposed to facilitate the conversion of rating factors between ASR and LRFR as a function of the present condition of constructed timber bridges.

17. Key Word	18. Distribution Statement
load and resistance factor design, load factor, stresses, timber construction, wooden bridges	Public distribution

19. Security Classif. (of this report)	20. Security Classif. (of this page)	21. No. of Pages	22. Price
Unclassified	Unclassified	40	n/a

Transition of Allowable Stress Rating to Load and Resistance Factor Rating for Timber Bridges

Yail Jimmy Kim, Ph.D., P.Eng., FACI

Department of Civil Engineering
University of Colorado Denver
Denver, Colorado

August 2024

Acknowledgments

The Principal Investigator gratefully acknowledges all individuals who contributed to the present research report.

Disclaimer

EXECUTIVE SUMMARY

This report presents the relevancy of the allowable stress rating (ASR) and the load and resistance factor rating (LRFR) methods for timber bridges. Benchmark bridges constructed in the 1930s have been upgraded with hollow structural steel (HSS) beams and three-dimensional finite element models provide technical information necessary for examining their behavior and rating evaluations. Complying with published manuals, 17 rating vehicles are considered across three categories (design, legal, and permit) to generate the maximum responses of the bridges. The vehicles' position dominates the deflection profiles of the unrepaired bridges. After installing the HSS beams, the live loads are redistributed, and stiffness enhancement is noticed in the transverse direction of the bridges. The rating factors calculated with ASR exceed those with LRFR for the unrepaired bridges regardless of vehicle configurations, and the level of disparity between these rating approaches increases when the bridges are repaired owing to differences in load factors. In terms of sensitivity to average daily truck traffic, the LRFR factors of the bridges under the "legal" vehicles are more responsive than the factors subjected to other vehicle types. From a probability perspective, the compatibility of these rating methodologies varies contingent upon vehicle categories and the presence of the HSS beams. Practice guidelines are proposed to facilitate the conversion of rating factors between ASR and LRFR as a function of the present condition of constructed timber bridges.

TABLE OF CONTENTS

LIST OF TABLES

LIST OF FIGURES

1. INTRODUCTION

As evidenced by the amended Fixing America's Surface Transportation Act (FAST Act) (US DOT 2016), limiting vehicle weights is a national interest to preserve highway bridge conditions. Constructed bridges suffer a wide variety of distress resulting from overloads, aggressive environments, collision, and fatigue (Shmerling and Catbas 2009; Dayan et al. 2022). Therefore, adequate assessments of in-situ bridges are indispensable to warrant the safe operation of civil infrastructure; bridge engineers actively seek technical solutions that can address pressing issues (ASCE/SEI-AASHTO 2009). Among other types of materials, timber was predominantly used for short-span bridges in the early 20th century. For example, more than 350 timber bridges were erected in the State of Colorado (4% of the total bridges) and most of them were in service for more than 50 years (FHWA 2022). Timber provides many advantages, such as abundant resources, environmental friendliness, amenity, affordable cost, and reduced labor; but it also has drawbacks like biological deterioration, fire vulnerability, low stiffness, and brittle failure (Kremer and Symmons 2015; Austigard and Mattsson 2020; Takeuchi et al. 2022). From a mechanical standpoint, overloading causes service and strength problems in timber bridges (Rashidi et al. 2021) and a catastrophic collapse may occur as in the case of the Tretten Bridge, Gudbrandsdalen Valley, Norway, in 2022 (Demirlioglu and Erduran 2024).

All bridges in the United States are inspected every two years and, pursuant to the Code of Federal Regulations (NARA 2022), new and existing bridges are subjected to load rating. The ratings are intended to identify a load level that a bridge can accommodate without excessive stress, which is an important task to effectively control the safety of structural members. Two rating categories are available for practice (AASHTO 2017): the inventory rating is intended to represent circumstances belonging to customary bridge design and to determine a live load that can be allowed for an indefinite period of time. By contrast, the operating rating is related to the maximum permissible live load a bridge carries. In the context of methodologies, the allowable stress rating (ASR) and the load and resistance factor rating (LRFR) methods are widespread (Stieglitz et al. 2022). The fundamental difference between ASR and LRFR is that the former is formulated deterministically, while the latter is probabilistically. The American Association of State Highway and Transportation Officials (AASHTO) Manual for Bridge Evaluation (AASHTO 2017) allows both ASR and LRFR for timber bridges, whereas no guidance is offered regarding which one is relevant to a certain situation. States like Colorado, Connecticut, Minnesota, and Washington enforce the use of ASR; nonetheless, LRFR is adopted by several states (e.g., Arizona, Iowa, and Florida) and some states do not employ ASR (e.g., Delaware and Nevada). Such a trend in acceptable rating methods signifies that there are transitional endeavors from ASR to LRFR when dealing with timber bridges, reminiscent of the shift from the AASHTO Standard Specifications to the AASHTO Load and Resistance Factor Design (LRFD) Bridge Design Specifications decades ago. Therefore, a systematic study is essential to holistically elucidate the applicability of ASR and LRFR to timber bridges with an emphasis on underlying discrepancies and complementary aspects.

As previously stated, one of the critical challenges facing the infrastructure community is that transportation agencies do not have sufficient information as to whether ASR furnishes a better rating for timber bridges compared with LRFR or vice versa. Simple arithmetic calculations will merely generate rating factors without knowing the actual performance of timber bridges. Refined investigations are, thus, necessary for handling this practical matter so as to advance state-of-the-art bridge rating technologies. The present paper discusses a comprehensive research program concerning the pertinence of ASR and LRFR to timber bridges under various vehicle loadings, including the implications of repair with steel beams, and suggests practice-oriented solutions. In so doing, bridge owners can properly manage built environments and efficiently spend funds on maintenance and traffic control.

2. RESEARCH SIGNIFICANCE

Since 2007, the Federal Highway Administration (FHWA) has mandated the load and resistance factor design (LRFD) method for all bridge structures; consequently, although not necessarily part of these requirements, bridge appraisals should be aligned with LRFR for consistency. However, the traditional allowable stress design (ASD) method is frequently adopted for timber bridges because most were constructed in accordance with the ASD method. Currently, there is no consensus on measuring the ability of a timber bridge to safely carry predetermined truck loads. The most notable concern is that a weight limit varies with rating methods, and state departments of transportation (DOTs) estimate the limit as per past experiences without scientific rationales. The research aims to clarify the technical appropriateness of ASR and LRFR through three-dimensional finite element analysis and to establish the foundation of understanding rating protocols for timber bridges.

3. BACKGROUND

3.1 Benchmark Bridges

According to communications with the Colorado Department of Transportation (CDOT), two timber bridges were chosen: one situated in Washington County (F-22-V) and the other in El Paso County (H-20-T). The three-span F-22-V bridge was erected in 1938 with 14 Douglas Fir girders with dimensions of 150-mm wide by 510-mm deep, as shown in Figure 1(a). The H-20-T bridge, built in 1935, had four spans consisting of 14 Douglas Fir girders with dimensions of 150-mm wide by 510-mm deep, as shown in Figure 1(b). The F-22-V bridge was straight, while the H-20-T bridge was skewed at an angle of 30°. The design vehicle at the time of construction was H15, which weighed 15 tons with two 4.3-m-spaced axles. The bridges' nominal properties, taken from the USDA Wood Handbook (USDA 2010), are listed in Table 1. Visual assessments were undertaken to examine the condition of these bridges, and an upgrade was recommended to improve their load-carrying capacities. As such, hollow structural steel (HSS) beams were placed adjacent to deteriorated girders for the purpose of repair, as seen in Figure 1(c). The beams were ASTM A500C steel with an elastic modulus of E_s = 200 GPa alongside a yield strength of f_y = 345 MPa and a Poisson's ratio of μ_s = 0.3. The repair procedure is delineated in Kim et al. (2024).

3.2 Rating Vehicles

As instructed by the CDOT Rating Manual (CDOT 2022), three vehicle categories (design, legal, and permit) were employed to investigate the flexural behavior of the benchmark bridges and to calculate rating factors. The design category involved the standard live loads of AASHTO [HS20 and HL93, Figure 2(a)], and the legal category is composed of assorted non-conforming trucks [legal types, hauling, and emergency vehicles, Figure 2(b)]. The Colorado permit and modified tandem vehicles are the components of the permit category, as shown in Figure 2(c). Whereas the total weight of the live loads varied from 213 kN to 852 kN, the axle gage distance in the transverse direction and the truck width were identical at 1.8 m and 3.0 m, respectively (CDOT 2022).

4. COMPUTATIONAL MODELING

4.1 Model Development

A concise summary of model formulation is provided herein, with complete details accessible elsewhere (Kim 2023; Kim et al. 2024). Three-dimensional finite element models were developed to predict the behavior of the bridges, shown in Figure 3(a), which were validated against experimental data. Solid elements comprised three translational degrees of freedom per node. and shell and frame elements constituted six degrees of freedom per node (three translational and three rotational). For material modeling, orthotropic and isotropic stress-strain laws formed the basis of the timber (Table 1) and steel (ASTM A500C), respectively. Regarding laboratory testing [Figure 3(b)], salvaged bridge girders were prepared to have dimensions of 150 mm in width by 170 mm in depth by 3.3 m in length and were monotonically loaded with and without HSS beams at a reduced scale. The repaired girders' capacity increased by 156.2% relative to that of the unrepaired control girders, on average. The performance of the full-scale F-22-V bridge, seen in Figure 3(c), was also enhanced by the steel repair in terms of reliability and stiffening efficiency. Selected responses from the test and modeling are visible in Figures 3(d) and (e).

4.2 Response Prediction

Figures 4(a) and (b) exhibit the deflection of F-22-V subjected to HS20. When the unrepaired bridge was loaded in one lane, an asymmetric profile was evident; however, under two-lane loading, the trend shifted toward symmetry, as Figure 4(a) shows. This is consistent with the fact that deflections in slab-on-girder bridges are dominated by the position of loaded trucks (Ndong et al. 2023). As the bridge was repaired, the tendency of girder deflections altered due to the redistributed vehicle loadings, as seen in Figure 4(b). The flat profile observed under the two-lane loading case demonstrates the effectiveness of the repair method; specifically, the transverse-directional stiffness of the superstructure was considerably enhanced. An analogous propensity was noticed for the deflection of H-20-T, and its maximum deflections under the 17 live loads are depicted in Fig. 4(c). Two-lane loading caused 4.4% higher deflections, on average, compared with its one-lane counterpart. In addition, the average deflections of the permit vehicles (live load numbers 16 and 17 for the Colorado permit and modified tandem trucks, respectively) were greater than the deflections of the design and legal vehicles (live load numbers 1 to 15) by 139%. The remarkably heavy loads of the permit trucks [852 kN and 444 kN, Figure 2(c)] are responsible for the increased deflections, even if the Colorado permit vehicle was not fully loaded because the 23.3-m axle distance was longer than the 6.85-m bridge span. Care should thus be exercised when allowing these permit vehicles to cross timber bridges, particularly considering the serviceability limit state. Figure 4(d) shows the maximum deflections of the repaired H-20-T bridge normalized by those of the unrepaired state. Regardless of vehicle conformations, the repair reduced the maximum deflections by 15.6% and 15.7% (normalized deflections = 0.844 and 0.843) for the one-lane and two-lane loadings, respectively, on average.

4.3 Live Load Distribution

The live load distribution factors for the moment of the unrepaired H-20-T bridge under the above-mentioned vehicle loadings are collated in Figure 5. The one-lane load for the interior girders rendered governing values across the board. The influence of the total weight and axle-to-axle distance in each truck was negligible; as a result, the variation of the maximum distribution factors was narrow, ranging from 0.180 to 0.191. Figure 6 illustrates the distribution factors for the moment of the repaired H-20-T bridge, which were normalized by the unrepaired occasion factors for comparison. The distribution factor ratio of the bridge was virtually independent of the loading positions and vehicle types, implying that the HSS repair generated uniform consequences. The entire distribution factors of the unrepaired and repaired F-22-V and H-20-T bridges are enumerated in Tables 2 through 3 and plotted in Figure 7, where the applicability of existing analytical equations (Table 4) is evaluated against the model predictions. A common pattern found was that the wheel-load-based AASHTO ASD overestimated the distribution factors in comparison with the axle-load-based AASHTO LRFD [Figures 7(a) to (d)], especially apparent for the two-lane loaded scenarios [Figures 7(e) and (f)]. Advanced modeling techniques like finite element analysis appear to be instrumental for dealing with mixed loading events.

5. LOAD RATING

5.1 Rating Methodologies

Conforming to the AASHTO Manual for Bridge Evaluation (AASHTO 2017) and the CDOT Rating Manual (CDOT 2022), the safe live load capacity of highway bridges is computed by ASR (Eq. 1) and LRFR (Eq. 2)

$$RF_{ASR} = \frac{C - A_1 D}{A_2 L(1+I)} \tag{1}$$

$$RF_{LRFR} = \frac{\phi_s \phi_c \phi R_n - \gamma_{DC} DC - \gamma_{DW} DW \pm \gamma_p P}{\gamma_{LL}(LL + IM)} \tag{2}$$

where RF is the rating factor of the bridge; C is the capacity of the bridge; D and L are the dead and live load effects, respectively; I is the impact factor; A_1 and A_2 are the dead and live load factors, respectively ($A_1 = A_2 = 1.0$ for ASR); ϕ_s is the system factor ($\phi_s = 1.0$ for most girder bridges, AASHTO 2017); ϕ_c is the condition factor ($\phi_c = 1.0$, 0.95, and 0.85 for good, fair, and poor conditions, respectively, AASHTO 2017); ϕ is the strength reduction factor; R_n is the nominal resistance; γ_{DC} and γ_{DW} are the dead load factors ($\gamma_{DC} = 1.25$ and $\gamma_{DW} = 1.5$) for the structural components (DC) and wearing surface (DW), respectively; γ_p is the factor ($\gamma_p = 1.0$) for the permanent load (P); γ_{LL} is the live load factor (Table 5); and IM is the dynamic load allowance. As outlined in the manuals (AASHTO 2017; CDOT 2022), the I and IM factors were assigned a value of 0 for timber bridges, and the legal and permit vehicles are valid for the operating level only.

5.2 Base Strength of Timber

The capacity of timber bridges may be calculated using (AASHTO 2002; AASHTO 2017; AASHTO 2020)

$$F_{B\text{-}ASR} = F_r C_D C_M C_t C_L C_F C_{fu} C_i C_r \tag{3}$$

$$F_{V\text{-}ASR} = F_{V0} C_D C_M C_t C_i \tag{4}$$

$$F_{B\text{-}LRFR} = F_r C_{KF} C_M C_{fu} C_i C_d C_\lambda \tag{5}$$

$$F_{V\text{-}LRFR} = F_{V0} C_{KF} C_M C_i C_\lambda \tag{6}$$

where F_B and F_V are the flexural and shear strengths of the timber, respectively; F_r and F_{V0} are the default strength of the timber for flexure and shear, respectively; C_D is the load duration factor; C_M is the wet service factor; C_t is the temperature factor; C_L is the stability factor; C_F is the size factor; C_{fu} is the flat use factor; C_i is the incising factor; C_r is the repetitive use factor; C_{KF} is the format conversion factor; C_d is the deck factor; and C_λ is the time effect factor. For the F-22-V and H-20-T bridges, the duration and size factors were $C_D = 1.15$ (two months for cumulative live load effect) and $C_F = 0.94$ (girder depth = 510 mm) in Eqs. 3 and 4, respectively; the format and time effect factors in Eqs. 5 and 6 were $C_{KF} = 2.5/\phi$ and $C_\lambda = 0.8$, respectively, and all other factors were set to be unity (AASHTO 2017). The shear capacity of the girder ($V_{R\text{-}ASR}$ and $V_{R\text{-}LRFR}$) can be obtained from Eqs. 7 and 8 (AASHTO 2002; AASHTO 2020)

$$V_{R-ASR} = \frac{2}{3} F_{V-ASR} bd \tag{7}$$

$$V_{R-LRFR} = \frac{F_{V-LRFR} bd}{1.5} \tag{8}$$

where b and d are the width and depth of the girder, respectively. Regarding the repaired girders, the capacity adjustment factor (α_{adj}) is used (Kim et al. 2024)

$$\alpha_{adj} = \frac{I_{rep} y_0}{I_0 \left(h_w - y_{rep} \right)} \tag{9}$$

where I_{rep} and I_0 are the moment of inertia of the repaired and control sections, respectively; y_{rep} and y_0 are the distance from the neutral axis to the extreme tension fiber of the girder with and without the repair, respectively; and h_w is the height of the timber girder. The flexural (M_{rep}) and shear (F_{Veff}) capacities of the repaired bridge are then expressed as

$$M_{rep} = \frac{\left(\alpha_{adj} F_r \right) I_0}{y_0} = \frac{F_{Beff} I_0}{y_0} \tag{10}$$

$$F_{Veff} = 0.2 \left(\alpha_{adj} F_r \right)^{0.8} = 0.2 \left(F_{Beff} \right)^{0.8} \tag{11}$$

where F_{Beff} is the effective bending strength of the timber after the repair. For simulation purposes, the default properties of the timber in F-22-V and H-20-T were taken to be F_r = 11 MPa and 15 MPa and F_{VO} = 0.78 MPa and 1.03 MPa for the inventory and operating levels, respectively (CDOT 2022), along with average daily truck traffic (ADTT) ≥ 5,000 (Table 5) and the negligible contribution of wearing and permanent dead load components was not taken into account with ϕ_c = 0.85. The solved finite element models furnished the dead and live load effects of the benchmark bridges in line with the densities of 800 kg/m^3 and 7,850 kg/m^3 for the timber and steel beams, respectively (AASHTO 2020).

5.3 Comparison of Rating Factors

Figure 8 displays the rating factors of F-22-V before and after the repair. To efficaciously differentiate the implications of vehicle types, inventory and operating levels were separately graphed for the design and the legal and permit categories. The unrepaired bridge under the design loads showed a marginal increase in the operating level against the inventory level, and the ASR factors were 122.2% higher than the LRFR factors, on average [Figure 8(a)]. These slanted factors agree with the reliability indexes of β = 2.5 and 3.5 for the operating and inventory levels (AASHTO 2017); the former necessitates a lower level of safety since lifetime loading for existing bridges may not need to be the same as the conservative loading required for new structures (Moses 2001). The skewed inclination of the rating factors was maintained in the legal and permit loads, as shown in Figure 8(b). The ASR factors were 137.1% and 137.6% greater than the LRFR factors for flexure and shear, respectively, on average. The live load factors spanning from γ_{LL} = 1.15 to 1.8 (Table 5) resulted in the lower LRFR factors (Eq. 2) compared with the ASR factors, which were linked to the corresponding factor of A_2 = 1.0 in Eq. 1. Subsequent to the HSS repair, the disparity between ASR and LRFR became more pronounced with the increased degree of scatter, as seen in Figures 8(c) and (d). A plausible explanation for the elevated dispersion is that the divergence in the

upgraded girder capacities associated with these rating approaches was amplified by the LRFR load factors.

5.4 Effectiveness of Repair

The ratio of rating factors with and without the repair is charted in Figure 9. The efficacy of the strengthening work was obvious across the spectrum, whereas the individual responses of the bridges were contingent upon rating methodologies and capacity classifications. For F-22-V with ASR, the average flexural and shear rating ratios under the design loads were 1.72 and 2.33, respectively, and these ratios increased to 1.99 and 2.68 under the legal and permit loads [Figures 9(a) and (b)]. Contrary to the variable rating ratios of ASR, the LRFR ratios of H-22-V remained relatively steady with a range of 1.3 to 1.63, as Figures 9(a) and (b) indicate. Figures 9(c) and (d) show similar predispositions for H-20-T with average differentials of 1.48 and 2.34 (ASR) and 1.11 and 1.40 (LRFR) for flexure and shear, respectively. These observations denote that LRFR may provide more stable ratings for repaired timber bridges. Extended discussions are given in Figure 10, where the proportions of the ASR and LRFR ratings are emphasized. The normalized average rating factors (LRFR/ASR) of the unrepaired bridges were nearly constant at 0.84 and 0.73 for the design and the legal and permit loads, respectively. The repaired bridges revealed reduced average factors by 24.5% and 40.0% for flexure and shear, respectively, from the factors of the unrepaired ones. The noticeable discrepancy in shear is ascribed to the escalated ratings of ASR (Figure 9), reaffirming the adequacy of LRFR in ensuring consistent rating outcomes.

5.5 Effect of Traffic Volume

Because the high volume of truck traffic significantly contributes to bridge deterioration (Feroz and Dabous 2021), the ramifications of average daily truck traffic (ADTT) were examined. Figures 11(a) and (b) portray the rating factors for the unrepaired and repaired states of F-22-V, respectively, based on LRFR when exposed to ADTT of 100 to 5,000 (Table 5). Attention was paid to operating levels, highlighting the significance of the maximum permissible live load that timber bridges can withstand. Overall, the flexural rating factors of the bridge were positioned above the shear rating factors, and the magnitudes of the factors went up with a decrease in ADTT. These aspects point out that the bridge was strengthened for flexure primarily, and excessive live loadings can lessen its load-bearing capacities. To determine the dependency of live loads on ADTT, the rating factors of the repaired H-20-T bridge under the 17 vehicles were normalized by the standard live load factors of AASHTO LRFD (HL93) in Figure 11(c). The hauling vehicles (live load numbers 9 to 13) were most responsive to ADTT, followed by other legal vehicles (live load numbers 3 to 8), while the emergency and the permit vehicles (live load numbers 14 to 17) were insensitive. As shown in the average responses of the three categories [Figure 11(d)], caution is advised regarding timber bridges with substantial ADTT (e.g., > 1,000) being rated under the legal vehicles.

5.6 Probabilistic Compatibility

The equivalence of the rating factors attained from ASR and LRFR is probabilistically assessed in Figure 12. Complying with the literature (Nowak and Taylor 1986; Barker and Puckett 2021), the resistance of the timber bridges was assumed to be lognormal with a coefficient of variation of COV = 0.15. The graphical interpretation of the probability density functions epitomized in Figures 12(a) and (b) is that the overlapping area of the distributions [Figure 12(a) inset] manifests the mutual compatibility of the rating approaches, which is defined as characteristic probability. Specifically, the larger the intersected region of the distributions, the higher the similarity between ASR and LRFR. Findings indicate that the degree of disagreement ascended with the presence of the HSS beams, corroborated in the pre- and post-repair stages, as depicted in Figures 12(a) and (b), respectively. The characteristic probability of H-20-T for flexure is described in Figure 12(c), which is akin to that of F-22-V. The compatibility of the unrepaired bridge was lowest when subjected to the Colorado and interstate legal vehicles (live load numbers 3 to 8); contrarily, the emergency and permit vehicles (live load numbers 14 to 17) generated higher values up to 92.5%. The response pattern of the repaired bridge was retained with lower probabilities. As referred to in Figure 12(d), the average characteristic probabilities of the unrepaired bridge for flexure and shear were comparable; however, different configurations were noticed after installing the HSS beams. These facts mean that, on most occasions, rigorous computations should be conducted for rating timber bridges to comprehend the potential impact of ASR and LRFR unless alternative methods are available.

6. PRACTICE RECOMMENDATIONS

6.1 Conversion between LRFR and ASR

In practice, it is often necessary to switch between rating factors determined from one method to another for assisting with decision-making processes. Accordingly, multiple calculations are integral for practitioners to ascertain explicit solutions. An efficient transition mechanism could ease the execution of these routine tasks. With the intention of addressing such prevalent needs, a conversion factor (ψ) is proposed to be

$$\psi = \frac{RF_{ASR}}{RF_{LRFR}} \tag{12}$$

Substituting Eqs. 1 and 2 into Eq. 12,

$$\psi = \frac{\left(C - D\right)\gamma_{LL}}{\phi_s \phi_c \phi R_n - \gamma_{DL} DC} \tag{13}$$

Considering that the dead load effects of the timber bridges are negligible in comparison with the load-carrying capacity of the bridges (Nowak and Eamon 2005), Eq. 13 is simplified as

$$\psi_{simp} = k_1 \frac{C}{R_n} \tag{14}$$

where ψ_{simp} is the simplified conversion factor and k_1 is the performance constant ($k_1 = 2.05/\phi_c$ for flexure and $2.33/\phi_c$ for shear).

6.2 Implementation

The conversion factors of F-22-V under the rating vehicles were calculated with a condition factor of ϕ_c = 0.85 and are demonstrated in Figure 13(a). Stepwise categorization was recognized depending on the types of vehicles. The ψ factors for flexure and shear were indistinguishable before the repair; conversely, as the bridge was upgraded, the factors for shear consistently exceeded those for flexure by an average of 20.1%. Figure 13(b) sorts out the average conversion factors pertaining to the three vehicle categories. In contrast to the unrepaired state factors, higher factors were in demand for the repaired state. For instance, after installing the HSS beams, the factors for flexure and shear rose by 26.7% and 60.0%, respectively, on average. As shown in Figure 13(c), conversion factor ratios for F-22-V and H-20-T were almost invariable with and without the repair system, supporting the general applicability of the suggested approach. For implementation in practice, the exact and simplified factors (Eqs. 13 and 14, respectively) can be interchangeable as substantiated in Figure 13(d).

6.3 Proposal

In conformity with the condition factors (ϕ_c) and the rating vehicle categories specified in the aforementioned manuals (AASHTO 2017; CDOT 2022), the conversion factors were calculated and are particularized in Table 6. The decreased condition factors led to an increase in the ψ factors with a range of 0.87 to 1.23 and 1.21 to 2.45 for the unrepaired and repaired situations, respectively. The legal category exhibited the highest susceptibility to the condition factor, while the permit category was notably affected by the HSS repair.

7. SUMMARY AND CONCLUSIONS

This report has focused on the rating of timber bridges with and without HSS-beam repair. On the basis of previously performed laboratory and field tests plus finite element modeling, load effects were computed for two benchmark bridges utilizing three categories of 17 rating vehicles in conjunction with published rating manuals (AASHTO 2017; CDOT 2022): Design (HS20 and HL93), Legal (legal types, hauling, and emergency vehicles), and Permit (Colorado permit and modified tandem vehicles). Upon elucidating the flexural behavior of the bridges, live load-carrying capacities were quantified by the allowable stress rating (ASR) and the load and resistance factor rating (LRFR) methods. Furthermore, parametric studies were carried out to explore the repercussions of average daily truck traffic (ADTT), which is one of the principal factors degrading the performance of bridge structures. To facilitate a convenient transition from LRFR to ASR, a conversion factor was proposed. The following are concluded:

- The position of loaded vehicles influenced the deflection profiles of the unrepaired bridges, while the presence of the HSS beams redistributed the live loads and changed the layout with enhanced stiffness in the transverse direction. The permit vehicles induced greater deflections relative to the design and legal vehicles over 139%, justifying extra attention from a serviceability point of view.
- Without regard to the weight, axle distance, and type of the rating vehicles, live load distribution factors were steady for the bridges. The ratio of the distribution factors before and after the repair was not modified by the vehicles' location. The AASHTO ASD distribution factors surpassed those of AASHTO LRFD.
- The ASR factors showed a 122.2% elevation over the LRFR factors for the unrepaired bridges under the design loads, and the tendency was maintained under the legal and permit loads. When the bridges were repaired, the level of divergence increased between the rating approaches owing to their distinct load factors. Unlike the case of emergency and permit vehicles, the LRFR factors of the bridges loaded with the legal vehicles were susceptible to ADTT.
- The repaired bridges received steadier ratings with LRFR against ASR. As per the defined characteristic probability, the compatibility between the rating methodologies for the unrepaired bridges declined under the legal vehicles, and the installation of the HSS beams intensified the variation.
- The conversion factors of the unrepaired bridges were equivalent for flexure and shear; on the contrary, inconsistency in these factors became enlarged after the repair. Regardless of the repaired state, the conversion factor method proved to be universally adaptable. The tabulated factors can be chosen for practice at a desired condition factor, tailored to specific rating vehicles.

REFERENCES

AASHTO. 2002. *Standard Specifications for Highway Bridges* (17th edition), American Association of State Highway and Transportation Officials, Washington, D.C.

AASHTO. 2017. The *Manual for Bridge Evaluation* (3rd edition), American Association of State Highway and Transportation Officials, Washington, D.C.

AASHTO. 2020. *AASHTO LRFD Bridge Design Specifications* (9th edition), American Association of State Highway and Transportation Officials, Washington, D.C.

ASCE/SEI-AASHTO. 2009. "White paper on bridge inspection and rating," *Journal of Bridge Engineering*, 14(1), 1-5.

Austigard, M.S., and Mattsson, J. 2020. "Fungal damages in Norwegian massive timber elements – a case study, *Wood Material Science & Engineering*, 15(6), 326-334.

Barker, R.M., and Puckett, J.A. 2021. *Design of Highway Bridges: an LRFD Approach*, John Wiley & Sons, Hoboken, NJ.

CDOT. 2022. *Bridge Rating Manual*, Colorado Department of Transportation, Denver, CO.

Dayan, V., Chileshe, N., and Hassanli, R. 2022. "A scoping review of information-modeling development in bridge management systems," *Journal of Construction Engineering and Management*, 148(9), 03122006.

Demirlioglu, K., and Erduran, E. 2024. "Drive-by Bridge Damage Detection Using Continuous Wavelet Transform," *Applied Sciences*, 14(7), 2969.

Feroz, S., and Dabous, S.A. 2021. "UAV-based remote sensing applications for bridge condition assessment," *Remote Sensing*, 13(9), 1809.

FHWA. 2022. *National Bridge Inventory (NBI)*, Federal Highway Administration, Washington, D.C.

Kim, Y.J. 2023. "Structural strengthening of a constructed timber bridge: field application and numerical modeling," *Engineering Structures*, 288, 116003

Kim, Y.J., Wang, J., and Ji, Y. 2024. "Rating of constructed timber bridges repaired with steel beams," *Engineering Structures*, 303, 117469.

Kremer, P.D., and Symmons, M.A. 2015. "Mass timber construction as an alternative to concrete and steel in the Australia building industry: a PESTEL evaluation of the potential," *International Wood Products Journal*, 6(3), 138-147.

Moses, F. 2001. "Calibration of load factors for LRFR bridge evaluation," NCHRP Report 454, Transportation Research Board, Washington, D.C.

NARA. 2022. *Code of Federal Regulations: Title 23*, National Archives and Records Administration, College Park, MD.

Ndong, A.K., Sherif, M.M., Kassner, B., Ozbulut, O., and Harris, D.K. 2023. “Refined analysis of steel girder bridges for computation of live load distribution factors considering effects of freight and emergency vehicles,” *Engineering Structures*, 293, 116630.

Nowak, A.S., and Taylor, R.J. 1986. “Ultimate strength of timber-deck bridges,” *Transportation Research Record*, 1053, 26-30.

Nowak, A.S., and Eamon, C.D. “Load and resistance factor calibration for wood bridges,” *Journal of Bridge Engineering*, 10(6), 636-642.

Rashidi, M., Hoshyar, A.N., Smith, L., Samali, B., and Siddique, R. 2021. “A comprehensive taxonomy for structure and material deficiencies, preventions and remedies of timber bridges,” *Journal of Building Engineering*, 34, 101624.

Shmerling, R.Z., and Catbas, F.N. 2009. “Load Rating and Reliability Analysis of an Aerial Guideway Structure for Condition Assessment,” *Journal of Bridge Engineering*, 14(4), 247-256.

Stieglitz, M., Terzioglu, T., Hueste, M.B.D., Hurlebaus, S., Mander, J.B., and Paal, S.G. 2022. “Field Testing and Refined Load Rating of a Load-Posted Continuous Steel Girder Bridge,” *Journal of Bridge Engineering* 27(10), 05022008.

Takeuchi, T., Terazawa, Y., Komuro, S., Kurata, T., and Sitler, B. 2022, “Performance and failure modes of mass timber buckling-restrained braces under cyclic loading,” *Engineering Structures*, 266, 114462.

USDA. 2010. *Wood handbook: Wood as an engineering material*, United States Department of Agriculture, Madison, WI.

US DOT. 2016. “Load Rating for the FAST Act’s Emergency Vehicles,” US Department of Transportation, Washington, D.C.

Table 1. Mechanical properties of Douglas Fir

Property	Direction	Value
Elastic modulus (E)	Longitudinal	10,800 MPa
	Tangential	540 MPa
	Radial	734 MPa
Shear modulus (G)	Longitudinal-Tangential	842 MPa
	Tangential-Radial	76 MPa
	Longitudinal-Radial	691 MPa
Poisson's ratio (μ)	Longitudinal-Tangential	0.029
	Tangential-Radial	0.374
	Longitudinal-Radial	0.292
Modulus of rupture (MOR)	Longitudinal	53 MPa

Table 2. Live distribution factors for moment from finite element analysis: without repair

Vehicle	F-22-V				H-20-T			
	One-lane loaded		Two-lane loaded		One-lane loaded		Two-lane loaded	
	Interior	Exterior	Interior	Exterior	Interior	Exterior	Interior	Exterior
HS20	0.181	0.151	0.092	0.075	0.186	0.163	0.092	0.087
HL93	0.181	0.151	0.092	0.075	0.186	0.163	0.092	0.087
Colorado Legal Type 3	0.195	0.142	0.099	0.071	0.187	0.165	0.099	0.088
Colorado Legal Type 3S2	0.195	0.142	0.099	0.071	0.187	0.165	0.099	0.088
Colorado Legal Type 3-2	0.195	0.142	0.099	0.071	0.187	0.166	0.099	0.089
Interstate Legal Type 3	0.195	0.142	0.099	0.071	0.187	0.165	0.099	0.088
Interstate Legal Type 3S2	0.195	0.142	0.099	0.071	0.187	0.166	0.099	0.089
Interstate Legal Type 3-2	0.195	0.142	0.099	0.071	0.187	0.166	0.099	0.089
Hauling Vehicle A	0.179	0.152	0.090	0.076	0.184	0.164	0.090	0.088
Hauling Vehicle SU4	0.180	0.151	0.091	0.076	0.187	0.163	0.091	0.087
Hauling Vehicle SU5	0.179	0.152	0.091	0.076	0.186	0.164	0.091	0.088
Hauling Vehicle SU6	0.179	0.152	0.090	0.076	0.185	0.164	0.090	0.087
Hauling Vehicle SU7	0.179	0.152	0.090	0.076	0.184	0.165	0.090	0.088
Emergency Vehicle 2	0.181	0.151	0.092	0.076	0.191	0.161	0.092	0.087
Emergency Vehicle 3	0.180	0.151	0.091	0.075	0.187	0.166	0.091	0.089
Colorado Permit Truck	0.194	0.143	0.098	0.072	0.180	0.170	0.098	0.091
Colorado Mod. Tandem	0.195	0.142	0.099	0.071	0.186	0.164	0.099	0.088

Table 3. Live distribution factors for moment from finite element analysis: with repair

Vehicle	F-22-V				H-20-T			
	One-lane loaded		Two-lane loaded		One-lane loaded		Two-lane loaded	
	Interior	Exterior	Interior	Exterior	Interior	Exterior	Interior	Exterior
HS20	0.143	0.155	0.080	0.074	0.184	0.172	0.098	0.092
HL93	0.145	0.156	0.081	0.085	0.186	0.176	0.099	0.094
Colorado Legal Type 3	0.147	0.159	0.081	0.085	0.187	0.177	0.100	0.095
Colorado Legal Type 3S2	0.147	0.159	0.081	0.085	0.186	0.177	0.099	0.095
Colorado Legal Type 3-2	0.147	0.159	0.081	0.085	0.187	0.178	0.100	0.095
Interstate Legal Type 3	0.147	0.159	0.081	0.085	0.187	0.177	0.100	0.095
Interstate Legal Type 3S2	0.147	0.159	0.081	0.085	0.187	0.178	0.100	0.095
Interstate Legal Type 3-2	0.147	0.159	0.081	0.085	0.187	0.177	0.100	0.095
Hauling Vehicle A	0.146	0.158	0.080	0.084	0.185	0.177	0.099	0.094
Hauling Vehicle SU4	0.147	0.159	0.081	0.085	0.186	0.175	0.099	0.094
Hauling Vehicle SU5	0.146	0.158	0.080	0.085	0.185	0.176	0.099	0.094
Hauling Vehicle SU6	0.146	0.158	0.080	0.084	0.186	0.176	0.099	0.094
Hauling Vehicle SU7	0.146	0.158	0.080	0.084	0.186	0.177	0.099	0.095
Emergency Vehicle 2	0.147	0.159	0.082	0.085	0.182	0.174	0.098	0.094
Emergency Vehicle 3	0.147	0.159	0.081	0.085	0.186	0.179	0.099	0.096
Colorado Permit Truck	0.146	0.159	0.080	0.085	0.188	0.183	0.100	0.098
Colorado Mod. Tandem	0.146	0.159	0.081	0.085	0.186	0.176	0.100	0.095

Table 4. Live load distribution factors based on published specifications

Method	Girder	Loading	Equation
AASHTO ASD (AASHTO 2002)	Interior	One-lane loaded	*S*/1.22 for Metric and *S*/4 for US
		Two-lane loaded	*S*/1.14 for Metric and *S*/3.75 for US
	Exterior	One-lane loaded	Lever rule
		Two-lane loaded	Lever rule
AASHTO LRFD (AASHTO 2020)	Interior	One-lane loaded	*S*/2.04 for Metric and *S*/6.7 for US
		Two-lane loaded	*S*/2.29 for Metric and *S*/7.5 for US
	Exterior	One-lane loaded	Lever rule
		Two-lane loaded	Lever rule

Metric = SI units in meters; US = US customary units in feet

Table 5. Summary of live load factors for LRFR based on AASHTO (2017)

Rating category	Load type	Live load factor (γ_{LL})
Design load rating	HL-93	Inventory: 1.75 Operating: 1.35
Legal load rating	Routine commercial traffic: Type 3, Type 3S2, Type 3-3	ADTT unknown: 1.8 ADTT ≥ 5,000: 1.80 ADTT = 1,000: 1.65 ADTT ≤ 100: 1.40
	Special hauling vehicles: NRL, SU4, SU5, SU6, and SU7	ADTT unknown: 1.6 ADTT ≥ 5,000: 1.60 ADTT = 1,000: 1.40 ADTT ≤ 100: 1.15
Permit load rating	Routine (unlimited trips)	ADTT > 5,000: 1.80 (permit weight < 45 ton) and 1.30 (permit weight ≥ 68 ton) ADTT = 1,000: 1.60 (permit weight < 45 ton) and 1.20 (permit weight ≥ 68 ton) ADTT < 100: 1.40 (permit weight < 45 ton) and 1.10 (permit weight ≥ 68 ton)
	Special (limited crossing)	Single trip (no other vehicles): 1.15 Single trip (mixed vehicles) ADTT > 5,000: 1.50 ADTT = 1,000: 1.40 ADTT< 100: 1.35 Multiple trips (mixed vehicles) ADTT > 5,000: 1.85 ADTT = 1,000: 1.75 ADTT< 100: 1.55

ADTT = average daily truck traffic; NRL = notional rating load; linear interpolation for other ADTT

Table 6. Proposed conversion factor (ψ) from LRFR to ASR

Condition factor (ϕ_c)	State	Type	Live load		
			Design	Legal	Permit
1.00 (Good)	Before repair	Flexure	1.02	1.23	0.87
		Shear	1.03	1.24	0.88
	After repair	Flexure	1.36	1.61	1.21
		Shear	1.60	1.92	1.27
0.95 (Fair)	Before repair	Flexure	1.08	1.30	0.92
		Shear	1.09	1.31	0.93
	After repair	Flexure	1.44	1.71	1.28
		Shear	1.80	2.17	1.54
0.85 (Poor)	Before repair	Flexure	1.22	1.47	1.04
		Shear	1.23	1.48	1.05
	After repair	Flexure	1.63	1.94	1.44
		Shear	2.04	2.45	1.74

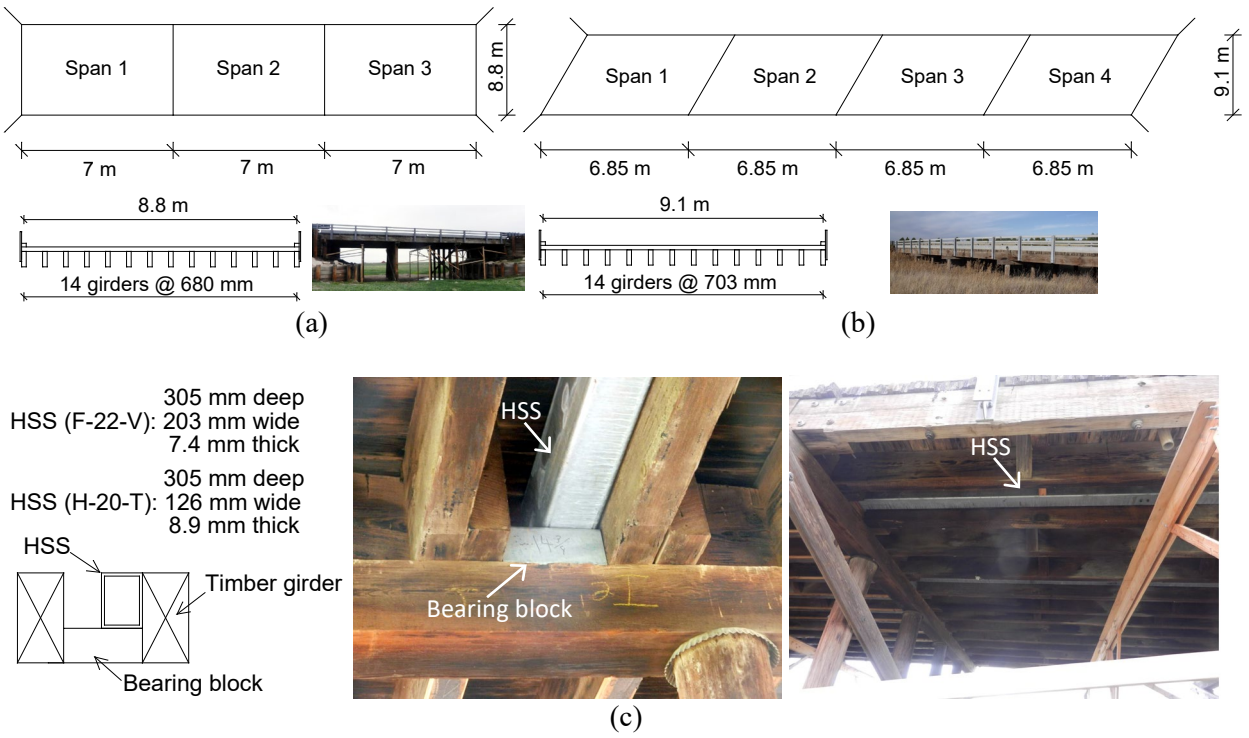

Figure 1. Benchmark bridges: (a) F-22-V; (b) H-20-T; (c) HSS-beam repair

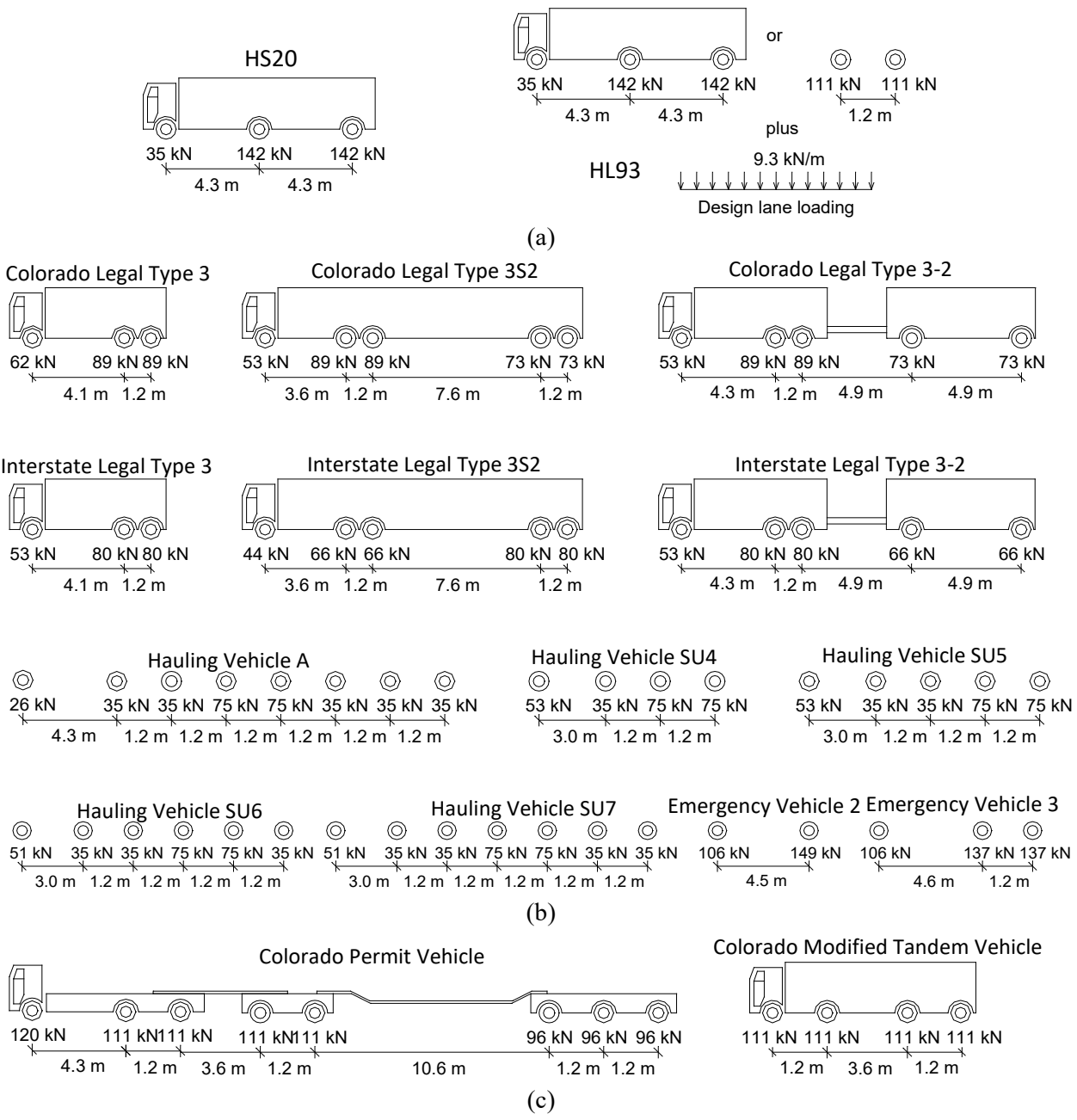

Figure 2. Rating vehicles: (a) Design; (b) Legal; (c) Permit

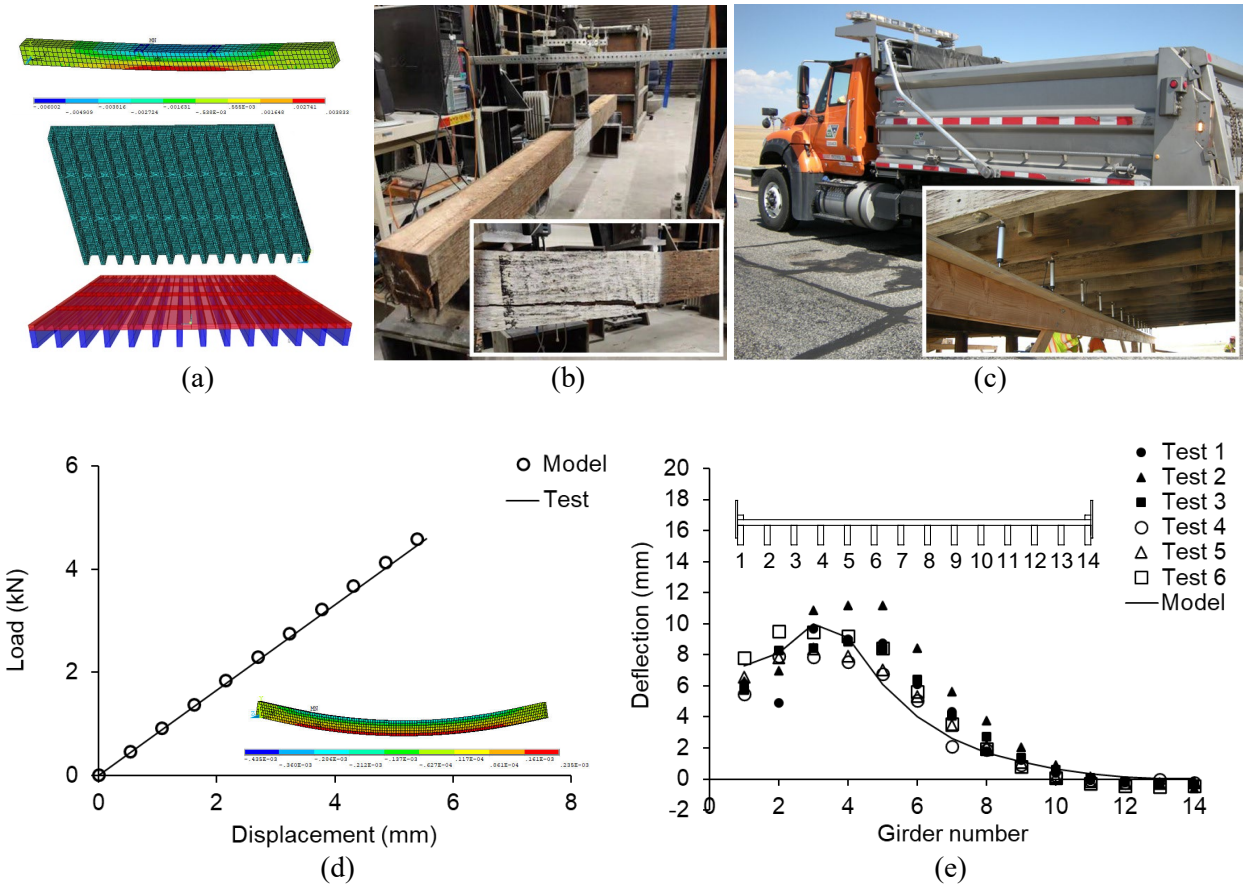

Figure 3. Model development: (a) computer models; (b) laboratory test; (c) field test; (d) validation of a single beam model; (e) validation of full-scale bridge model (F-22-V)

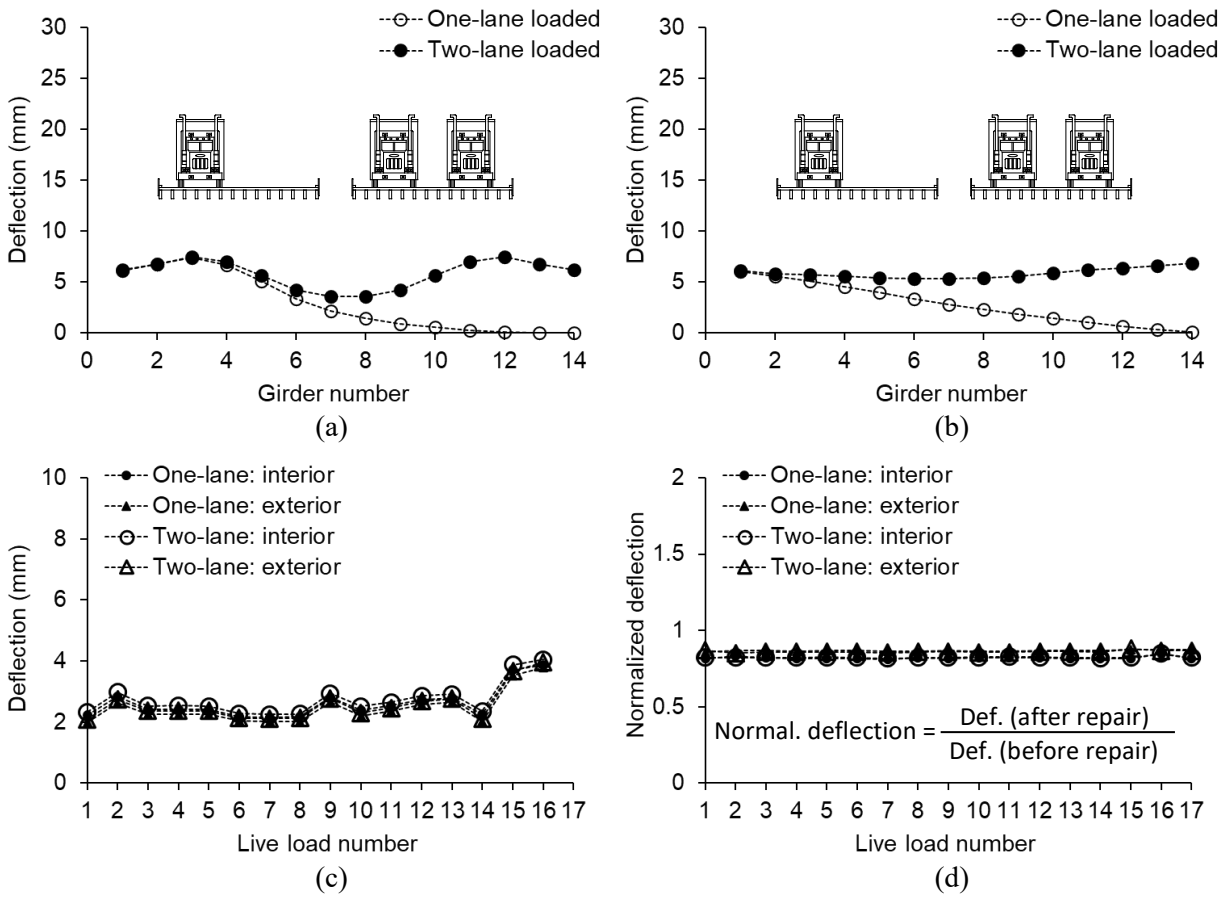

Figure 4. Deflection of bridges (Live load number: 1 = HS20; 2 = HL93; 3 = CO Legal 3; 4 = CO Legal 3S2; 5 = CO Legal 3-2; 6 = IS Legal 3; 7 = IS Legal 3S2; 8 = IS Legal 3-2; 9 = Hauling A; 10 = Hauling SU4; 11 = Hauling SU5; 12 = Hauling SU6; 13 = Hauling SU7; 14 = EV2; 15 = EV3; 16 = CO Permit; 17 = CO Modified Tandem): (a) unrepaired F-22-V under HS20; (b) repaired F-22-V under HS20; (c) maximum deflections of repaired H-20-T; (d) normalized maximum deflections of H-20-T

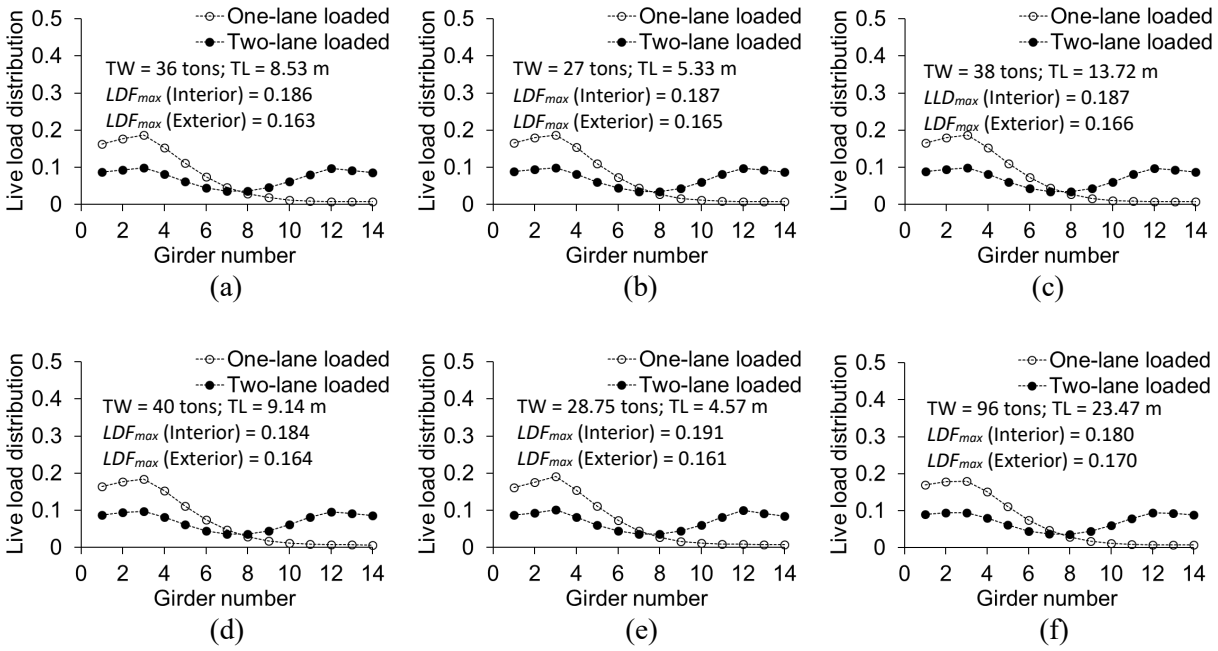

Figure 5. Live load distribution for moment of unrepaired H-20-T under selected vehicle loads (TW = truck weight in total; TL = truck length from front to rear axles): (a) HS20-44; (b) Colorado Legal Type 3; (c) Interstate Type 3S2; (d) Hauling Vehicle A; (e) Emergency Vehicle 2; (f) Colorado Permit

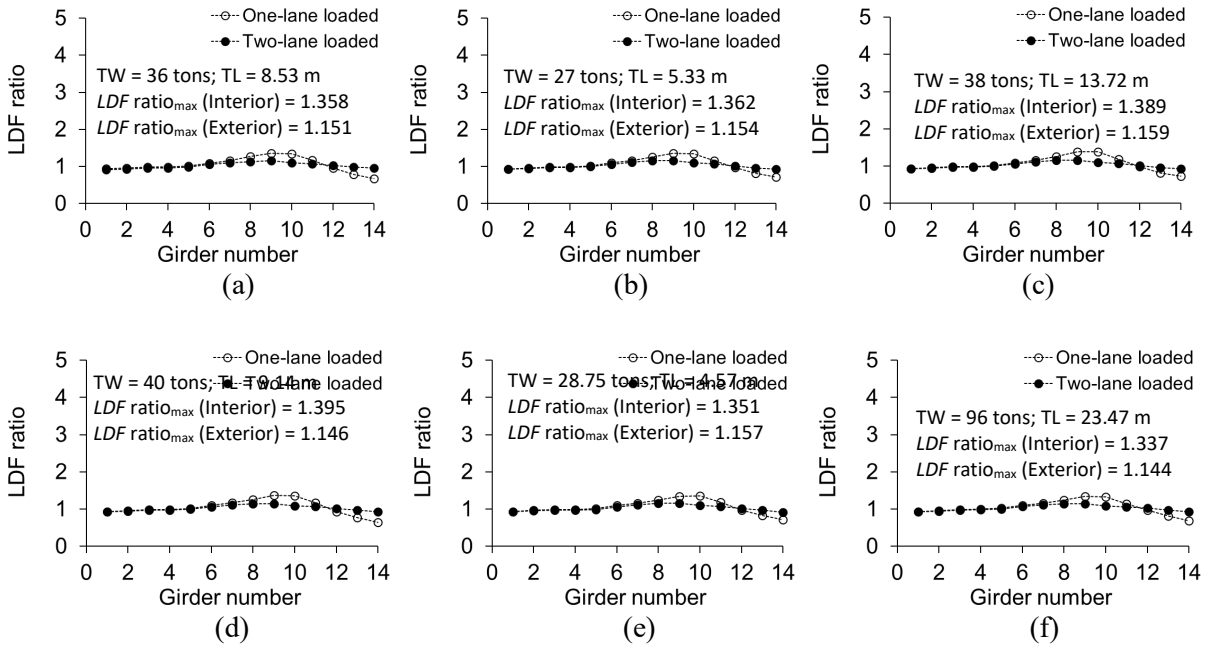

Figure 6. Live load distribution ratio for moment of repaired H-20-T under selected vehicle loads (TW = truck weight in total; TL = truck length from front to rear axles; LDF ratio = load distribution before repair/load distribution after repair): (a) HS20-44; (b) Colorado Legal Type 3; (c) Interstate Type 3S2; (d) Hauling Vehicle A; (e) Emergency Vehicle 2; (f) Colorado Permit

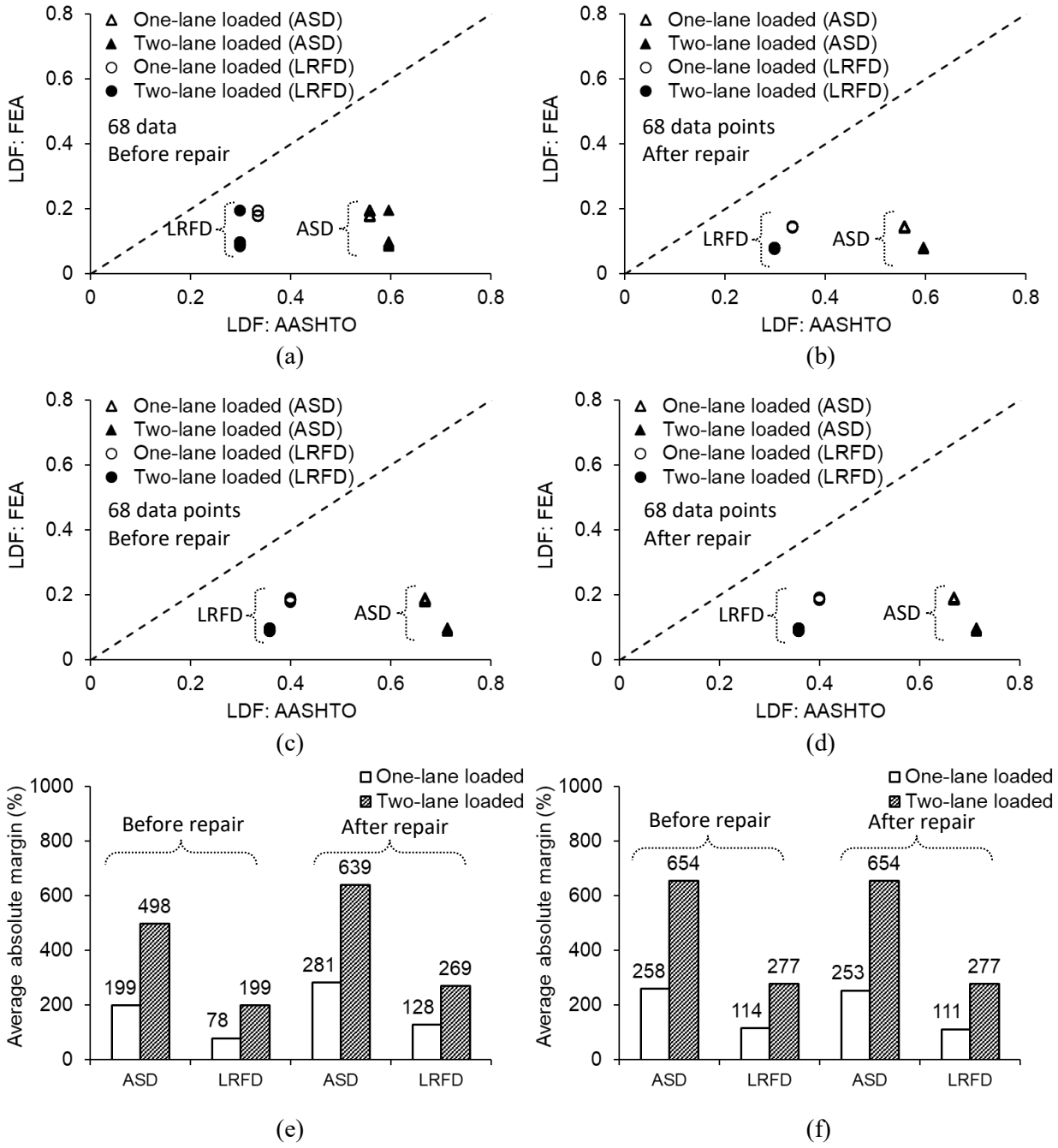

Figure 7. Comparison of live load distribution factors for moment of interior girders (LDF = load distribution factor; FEA = finite element analysis): (a) unrepaired F-22-V; (b) repaired F-22-V; (c) unrepaired H-20-T; (d) repaired H-20-T; (e) discrepancy of F-22-V; (f) discrepancy of H-20-T

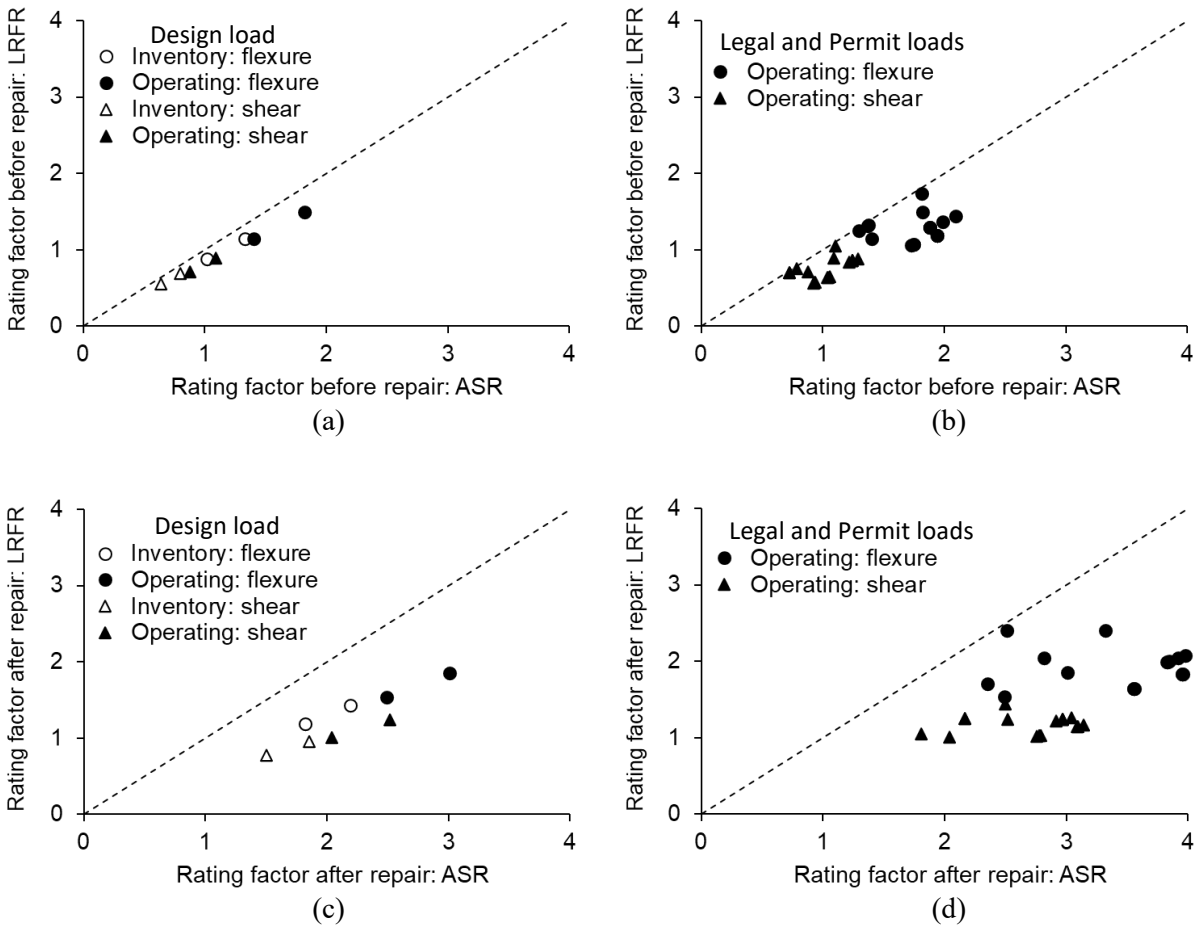

Figure 8. Comparison of rating factors between ASR and LRFR for F-22-V: (a) Design load before repair; (b) Legal and Permit loads before repair; (c) Design load after repair; (b) Legal and Permit loads after repair

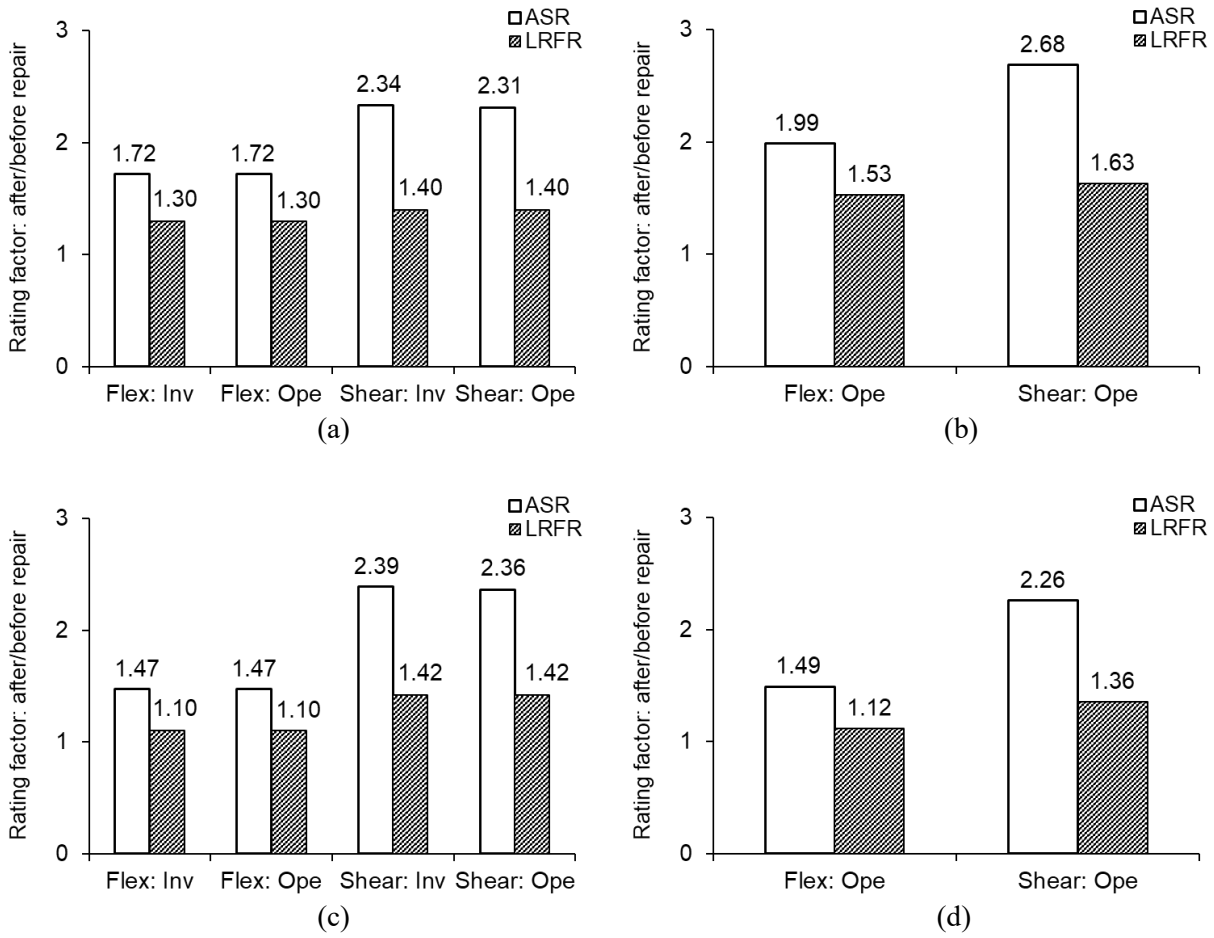

Figure 9. Effectiveness of repair (Flex = flexure; Inv = inventory; Ope = operating): (a) Design load for F-22-V; (b) Legal and Permit loads for F-22-V; (c) Design load for H-20-T; (d) Legal and Permit loads for H-20-T

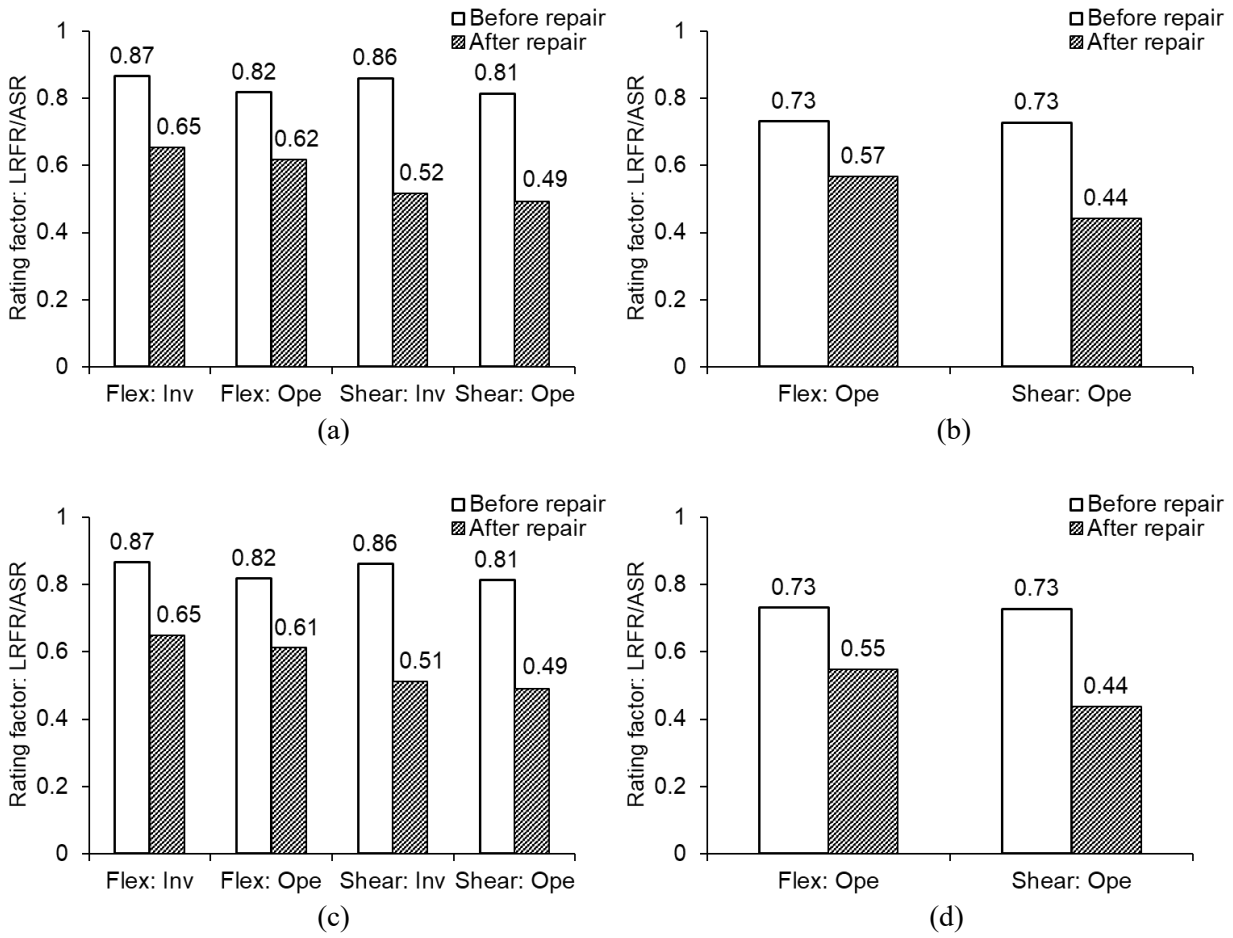

Figure 10. Assessment of ASR vs. LRFR (Flex = flexure; Inv = inventory; Ope = operating): (a) Design load for F-22-V; (b) Legal and Permit loads for F-22-V; (c) Design load for H-20-T; (d) Legal and Permit loads for H-20-T

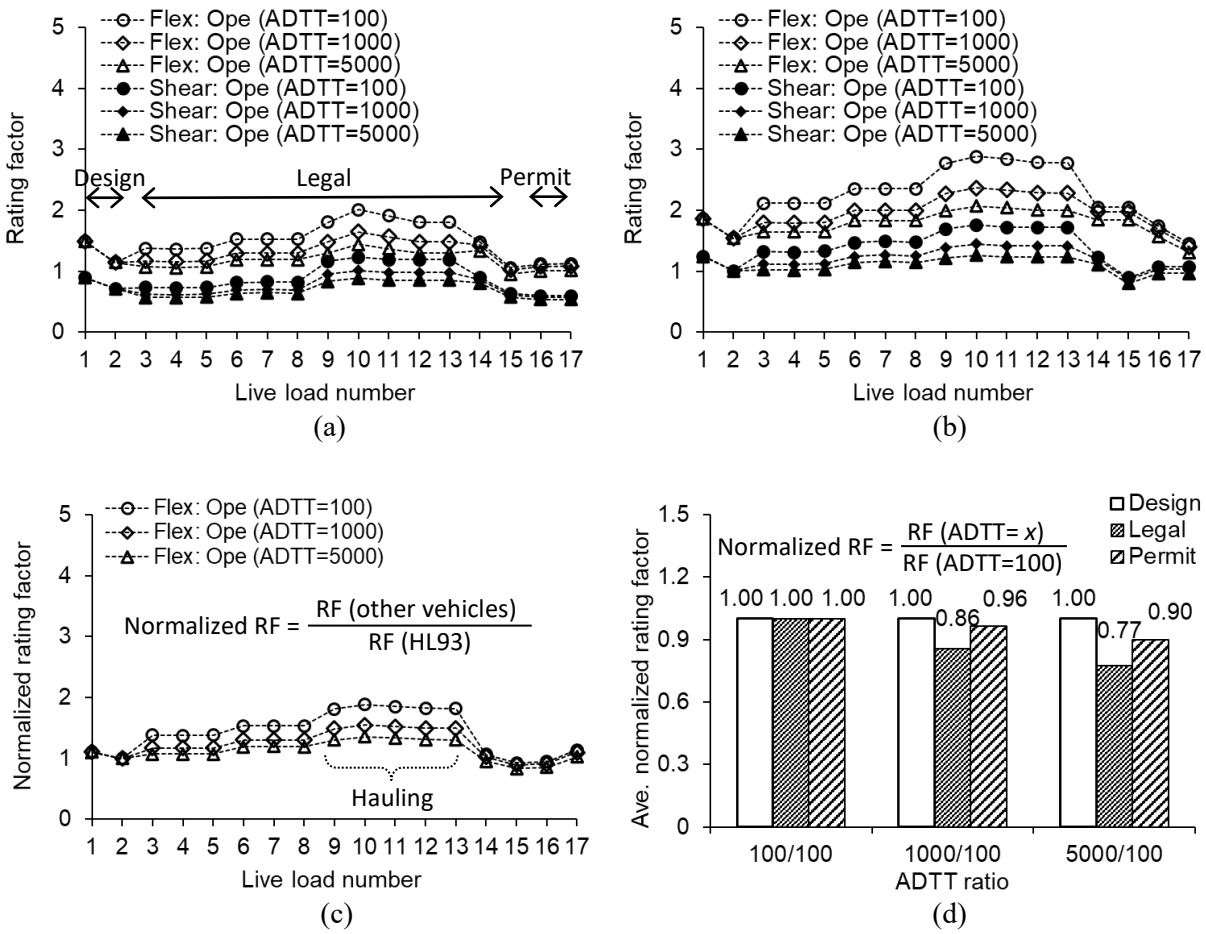

Figure 11. Parametric study (Live load number: 1 = HS20; 2 = HL93; 3 = CO Legal 3; 4 = CO Legal 3S2; 5 = CO Legal 3-2; 6 = IS Legal 3; 7 = IS Legal 3S2; 8 = IS Legal 3-2; 9 = Hauling A; 10 = Hauling SU4; 11 = Hauling SU5; 12 = Hauling SU6; 13 = Hauling SU7; 14 = EV2; 15 = EV3; 16 = CO Permit; 17 = CO Modified Tandem): (a) unrepaired F-22-V; (b) repaired F-22-V; (c) normalized rating factors of repaired H-20-T under HL93; (d) normalized rating factors of H-20-T for flexure with ADTT

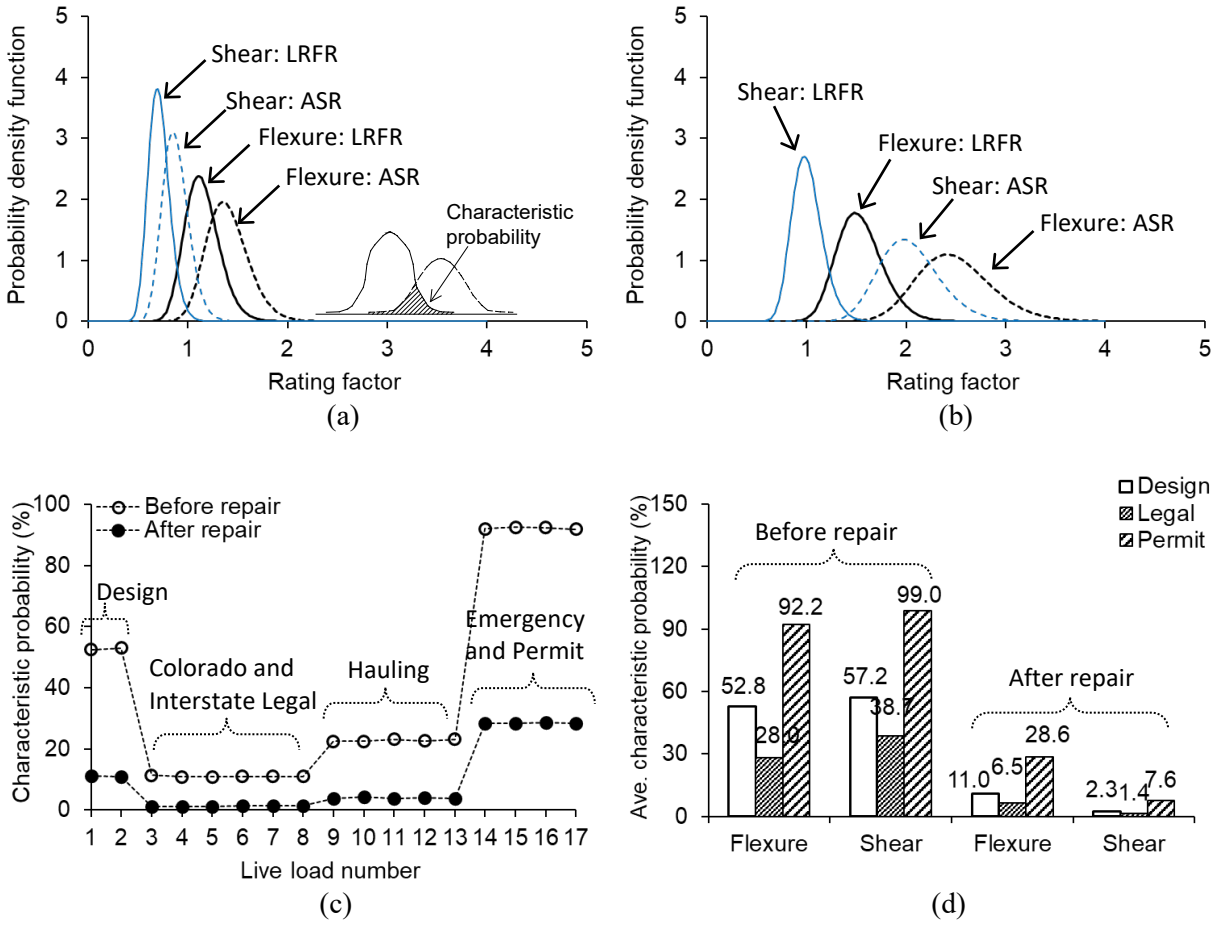

Figure 12. Probabilistic compatibility of timber bridges with operating rating (Live load number: 1 = HS20; 2 = HL93; 3 = CO Legal 3; 4 = CO Legal 3S2; 5 = CO Legal 3-2; 6 = IS Legal 3; 7 = IS Legal 3S2; 8 = IS Legal 3-2; 9 = Hauling A; 10 = Hauling SU4; 11 = Hauling SU5; 12 = Hauling SU6; 13 = Hauling SU7; 14 = EV2; 15 = EV3; 16 = CO Permit; 17 = CO Modified Tandem): (a) HL93 before repair of F-22-V; (b) HL93 after repair of F-22-V; (c) characteristic probability for flexure of H-20-T; (d) average characteristic probability before and after repair of H-20-T

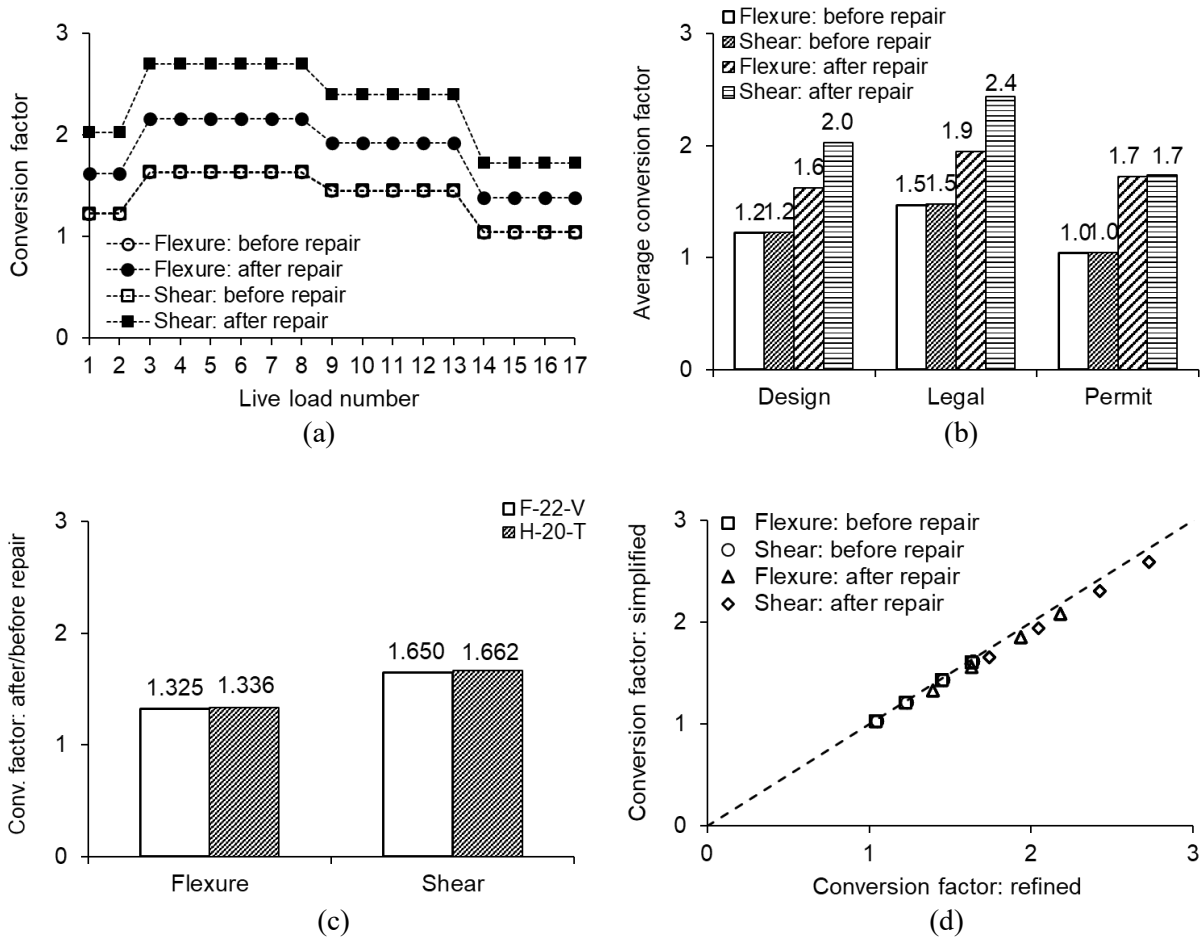

Figure 13. Conversion factor for operating rating with a condition factor of 0.85 (Live load number: 1 = HS20; 2 = HL93; 3 = CO Legal 3; 4 = CO Legal 3S2; 5 = CO Legal 3-2; 6 = IS Legal 3; 7 = IS Legal 3S2; 8 = IS Legal 3-2; 9 = Hauling A; 10 = Hauling SU4; 11 = Hauling SU5; 12 = Hauling SU6; 13 = Hauling SU7; 14 = EV2; 15 = EV3; 16 = CO Permit; 17 = CO Modified Tandem): (a) individual factors of F-22-V; (b) average normalized conversion factor of F-22-V with loading type; (c) average normalized conversion factor; (d) comparison between refined and simplified conversion factors of H-22-T